Investigation of the Photoreduction of Anthraquinonedisulfonic Acid by Triethylamine with Fourier Transform Electron Spin Resonance

J. Säuberlich, O. Brede, and D. Beckert*

Research Unit "Time Resolved Spectroscopy" at the University of Leipzig, Permoserstrasse 15, D-04303 Leipzig, Germany

Received: January 28, 1997; In Final Form: May 6, 1997[⊗]

The photoreduction of 9,10-anthraquinone-1,5-disulfonate and 9,10-anthraquinone-2,6-disulfonate with triethylamine in aqueous solution has been studied by laser photolysis using time-resolved Fourier transform electron spin resonance and optical detection in the nanosecond and microsecond time scale. With FT-ESR the semiquinone radical anions and the triethylamine radical cations could be detected at pH = 11 in Coulomb-coupled radical pairs in addition to the separated semiquinone radical anions. At pH = 14, the α-aminoalkyl radical could be detected as the decay product of the triethylamine radical cation. From the time dependence of the spin-polarized ESR intensities of the various components the lifetime of the Coulomb-coupled radical ion pair was determined. The radical ion pair decay exhibits a two-component behavior with a fast and a slow decay time. These lifetimes depend on the pH of the solution and are on the order of 10 ns to 2 μs.

Introduction

Since Fourier transform electron spin resonance (FT-ESR)[1−5] has been established in chemical reaction studies, the photoreduction of quinones by amines and phenols can be analyzed in more detail.[5−10] Whereas optical methods are appropriate for the study of the kinetics of reaction mechanisms[11−15] with high time resolution, the ESR technique is unique because it allows an analysis of the structure of the intermediate species. Using FT-ESR, the time resolution could be extended to the nanosecond range with full spectral resolution. Furthermore, the FT-ESR technique improves the sensitivity of time-resolved ESR.

Guttenplan and Cohen[16] first proposed that the primary reaction of the photoreduction was an electron transfer from amine in its ground state to the quinone triplet, forming a charge-transfer complex. These charge-transfer complexes can be changed to exciplexes, contact ion pairs, solvent-separated ion pairs, or free radicals, depending on the nature of the triplet state and the triplet quencher and solvent. A review dealing with the identification of transients and mechanisms in the photoreduction of quinones by amines was published by Cohen et al.[12]

Time-resolved ESR experiments in the nanosecond and microsecond time scale usually exploit the effects of chemically induced dynamic electron polarization (CIDEP).[17,18] The non-equilibrium spin polarization is generated by the triplet mechanism (TM) and/or the radical pair mechanism (RPM). The triplet polarization is produced by spin-selective intersystem crossing ($S_1 \rightarrow T_1$) of optically excited molecules, whereas the RPM changes the population of the two electron spin levels by the combined action of hyperfine interaction and exchange interaction within radical pairs. This RPM operates both during the initial separation of a geminate radical pair and also during random subsequent encounters in which the radicals recombine. Therefore, for an analysis of time-resolved ESR data one has to consider spin polarization, spin lattice relaxation to the Boltzmann magnetization, and the chemical kinetics.[7−10]

The reaction sequence in the photoreduction of quinone triplets by aliphatic amines can be described by the following scheme,[7,9,10,12] in which AQDS is used as an abbreviation for anthraquinone-1,5(2,6)-disulfonate and TEA for triethylamine, and spin-polarized radicals are denoted by *:

Excitation and intersystem crossing:

$$\mathrm{AQDS}_{So} \xrightarrow{h\nu} \mathrm{AQDS}_{S1} \xrightarrow{\mathrm{ISC}} \mathrm{AQDS}_{T1}^{*} \quad (1)$$

Spin−lattice relaxation of spin-polarized triplets:

$$\mathrm{AQDS}_{T1}^{*} \xrightarrow{^{3}T_1} \mathrm{AQDS}_{T1} \quad (2)$$

Electron transfer in encounter complex:

$$\mathrm{AQDS}_{T1}^{*} + \mathrm{TEA} \xrightarrow{k_{\mathrm{diff}}} \{\mathrm{AQDS}_{T1}^{*}\cdots\mathrm{TEA}\} \xrightarrow{k_{\mathrm{et}}} \{\mathrm{AQDS}^{\bullet -}{*}\cdots\mathrm{TEA}^{\bullet +}{*}\} \quad (3)$$

Escape from the solvent-separated ion pairs to free radical ions:

$$\{\mathrm{AQDS}^{\bullet -}{*}\cdots\mathrm{TEA}^{\bullet +}{*}\} \xrightarrow{k_{\mathrm{esc}}} \mathrm{AQDS}^{\bullet -}{*} + \mathrm{TEA}^{\bullet +}{*} \quad (4)$$

Deprotonation of radical cations:

$$\mathrm{TEA}^{\bullet +}{*} + \mathrm{OH}^{-} \rightarrow \mathrm{Et_2N{-}C^{\bullet}HCH_3}{*} + \mathrm{H_2O} \quad (5)$$

In this paper we describe the photoreduction of two derivatives of anthraquinone by triethylamine in aqueous solution detected by laser photolysis FT-ESR experiments. In these experiments we could detect the isolated anthraquinone radical anion in solution as well as the radical anion and the triethylamine radical cation as part of radical ion pair complexes in the time range 0.03−2.0 μs. This simultaneous and direct detection of both radical ions of the geminate pair generated by an electron-transfer reaction can be used to characterize the structure and kinetics of solvent-separated radical ion pairs.

Experimental Section

Laser photolysis experiments were performed with an excimer laser (Lambda Physik, LPX 105ESC; wavelength 308 nm; energy 10−15 mJ per pulse; pulse width 10 ns) for the FT-

* To whom correspondence should be addressed.

[⊗] Abstract published in *Advance ACS Abstracts,* July 15, 1997.

S1089-5639(97)00344-7 CCC: $14.00

ESR measurements and with a Nd^{3+}:YAG laser using the fourth harmonic with 266 nm (Spectra Physics Inc., Quanta Ray GCR-11; energy <10 mJ per pulse; pulse width 3 ns) for the laser flash experiments with optical detection.

FT-ESR spectra were recorded with a X-band home-built spectrometer described previously.[9] The cavity used is the Bruker split-ring module ER 4118 X-MS-5W. The microwave pulse is generated by a fast ECL-PIN diode with a rise time of 4 ns and amplified by a 1 kW traveling wave tube amplifier A710/X (LogiMetric, Inc.). The pulse width of a $\pi/2$ microwave pulse is 16 ns. The software for device control, data acquisition, and data analysis was developed in our institute. The experimental FID data were extrapolated into the dead time of the spectrometer (~100 ns) by the linear prediction singular value decomposition method (LPSVD),[22] which allows one to get spectra with a correct base line and correct intensities. The LPSVD program is described elsewhere.[19] The equipment for the optical absorption spectroscopy has been described previously.[20]

The experimental FT-ESR spectra are given in frequency units in relation to the spectrum center, where the g values are adjusted to the g value of the sulfite radical $SO_3^{\bullet-}$ with $g(SO_3^{\bullet-}) = 2.00316$.[21]

Materials. Anthraquinone-1,5(2,6)-disulfonic disodium salt and triethylamine (all from Aldrich) were used without further purification. Water was taken from an ultrapure water system milli-Q plus (Millipore). In order to avoid solute depletion by accumulated laser excitation and enrichment of photolytic reaction products, the solutions were flowing through the sample cell (quartz tube with an inner diameter of 1.5 mm) at a rate of approximately 1−2 mL/min. The flow system for the sample was assembled completely with glass tubing to ensure that oxygen could not diffuse into the sample solution between the bubbling vessel and the cavity. With this equipment we are able to remove oxygen to a concentration as low as 3×10^{-7} mol dm^{-3}.

Results

In Figure 1a,b the FT-ESR spectra of the 1,5-$AQDS^{\bullet 3-}$ and 2,6-$AQDS^{\bullet 3-}$ radical anions detected at a delay time of 2.0 μs after the laser pulse (pH = 11) are shown. All FT-ESR spectra shown in this paper are obtained by extrapolating missing time domain data using the LPSVD method.[22] The spectra of 1,5-$AQDS^{\bullet 3-}$ and 2,6-$AQDS^{\bullet 3-}$ are characterized by three sets of two equivalent protons, the coupling constants of the two derivatives deviating slightly. The coupling constants[23,24] are listed in Table 1. The radical anion spectra are emissively spin-polarized by the triplet mechanism with a small contribution of RPM polarization, which can be deduced from the small asymmetry in the spectra.

In addition to the quinone radical anions 1,5-$AQDS^{\bullet 3-}$ and 2,6-$AQDS^{\bullet 3-}$ we observe at short delay times six groups of lines separated by approximately 60 MHz. This spectrum is shown in Figure 2a and can be assigned to the TEA radical cation.[10,25,26] The simulated spectrum in Figure 2a was calculated with hfs coupling constants determined from ESR[26] and FDMR[25] measurements in the solid phase. In order to confirm this interpretation, the experiment was repeated with ^{15}N-substituted TEA, and the result is shown in Figure 2b. The coupling constants change as predicted by using the ratio of the nuclear g values of $g(^{15}N)/g(^{14}N) = 1.402$ (cf. Table 1). Both spectra (Figure 2a,b) are emissively spin-polarized (TM) with an RPM contribution larger than in the radical anion spectra. This is in agreement with the larger coupling constants of the radical cations.

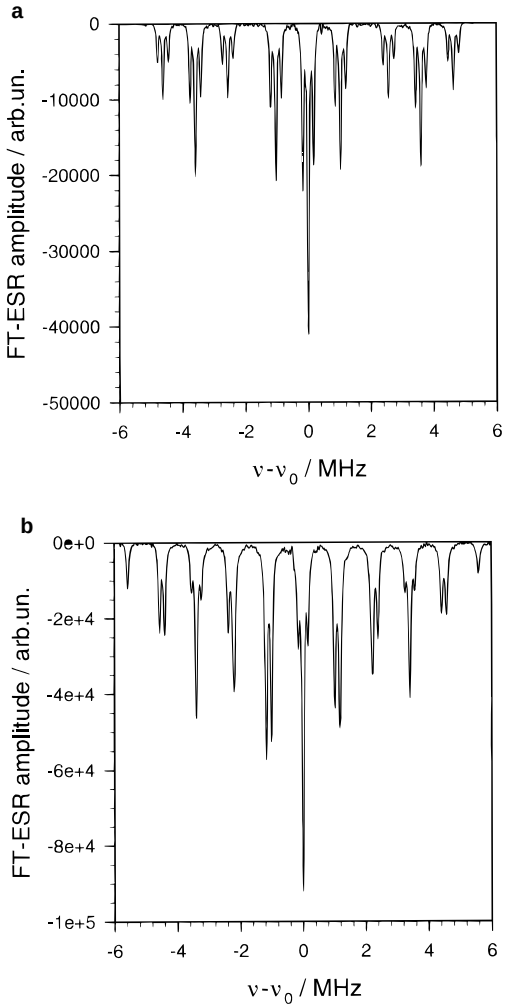

Figure 1. FT-ESR spectra of (a) 1,5-$AQDS^{\bullet 3-}$ and (b) 2,6-$AQDS^{\bullet 3-}$ radical anions after a delay of 2 μs from the laser pulse. The free induction decays were extrapolated in the dead time by the LPSVD method. Sample: 1 mM AQDS with 30 mM TEA in aqueous solution with pH = 11. Laser energy per pulse: 15 mJ.

In Figure 3a,b the FT-ESR spectra of 1,5-$AQDS^{\bullet 3-}$ and 2,6-$AQDS^{\bullet 3-}$ are shown for short delay times ($\tau_{del} = 32$ ns). Two characteristic features, an essential lower spectral intensity and a broad background at each line position, are obvious. The dependence of the FT-ESR intensity on the delay time will be discussed in detail below. The broad lines at exactly the same positions as found for the narrow lines (cf. Figure 1a,b) are not caused by an incorrect extrapolation of the free induction decay but originate from radical anions 1,5-$AQDS^{\bullet 3-}$ and 2,6-$AQDS^{\bullet 3-}$ in close contact with the radical cations $TEA^{\bullet +}$ within Coulomb-coupled pairs.[7−10] The quantitative separation of these two contributions is shown in Figure 4, in which the simulated spectrum is the superposition of two radicals with the same hfs coupling constants but different line widths. The narrow line spectrum was calculated with a fwhm line width of 84 kHz and the broad line one with 900 kHz. In the same way all spectra were analyzed as a function of the delay time. The total FT-ESR intensities of both contributions are represented in Figure 5a for 1,5-$AQDS^{\bullet 3-}$ and in Figure 5b for 2,6-$AQDS^{\bullet 3-}$. The time dependence of the 1,5(2,6)-$AQDS^{\bullet 3-}$ intensities can be simulated using the empirical function

$$I(t) = [m_0 + m_1(1 - \exp(-k_{esc}t))][(P - 1)\exp(-t/T_1) + 1] \quad (6)$$

in which the first bracket describes the buildup kinetics of the

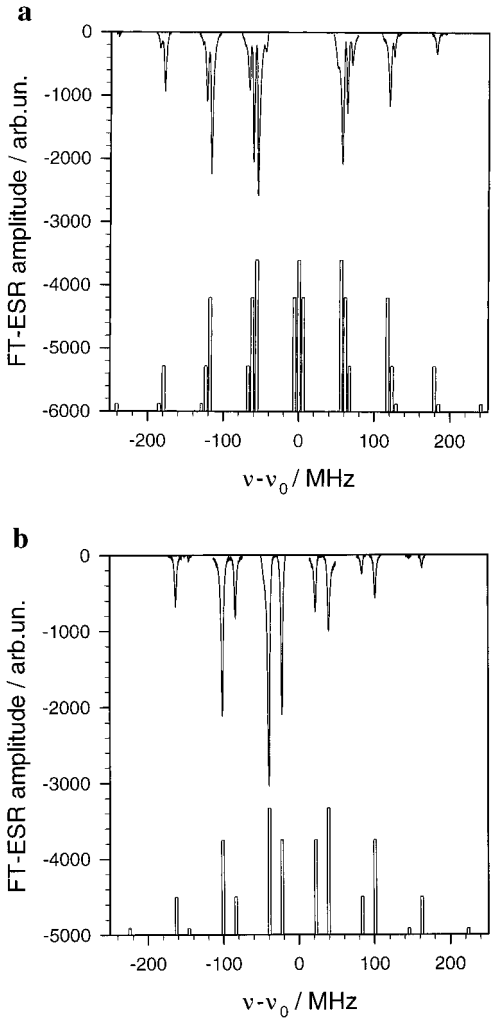

Figure 2. FT-ESR spectra of (a) ^{14}N-TEA and (b) ^{15}N-TEA radical cation after a delay time of 0.1 μs compared with the simulated spectra (hfs coupling constants see Table 1). Sample: 1 mM 2,6-AQDS with 30 mM TEA in aqueous solution. Laser energy per pulse as in Figure 1 but 4 times more repetitons in data aquisition.

TABLE 1: Spectroscopic Parameters of 1,5-AQDS$^{\bullet 3-}$ and 2,6-AQDS$^{\bullet 3-}$ Radical Anions in Free State and Pair State and of the TEA$^{\bullet +}$ Radical Cation and the Aminoalkyl Radical $(CH_3CH_2)_2N-C^{\bullet}H-CH_3$ in Aqueous Solution; The Error Limits Are Indicated in Parentheses in Units of the Last Digit

radical	*g* factor	hfs coupling constants [MHz]	line width [kHz]
1,5-AQDS$^{\bullet 3-}$	2.0042(2)	a(2H,3,7) = 3.60(2)	
(free state and		a(2H,4,8) = 1.03(2)	84 ± 5 (free state)
pair state)		a(2H,2,6) = 0.17(1)	900 ± 100 (pair)
2,6-AQDS$^{\bullet 3-}$	2.0041(2)	a(2H,3,7) = 3.40(5)	
(free state and		a(2H,1,5) = 1.17(1)	84 ± 5 (free state)
pair state)		a(2H,4,8) = 1.01(3)	900 ± 100 (pair)
TEA$^{\bullet +}$	2.0038(1)	a(N) = 56.(1)	(2.5 ± 0.2) × 10^3
(^{14}N)		a(6H,β) = 62.(3)	
TEA$^{\bullet +}$	2.0038(0)	a(N) = 79.(4)	(2.5 ± 0.2) × 10^3
(^{15}N)		a(6H,β) = 62.(0)	
$Et_2N-C^{\bullet}HCH_3$	2.0033(2)	a_α(1H) = 39.(1)	(2.8 ± 0.3) × 10^3
		a_β(3H) = 53.(9)	
		a_γ(4H) = 7.1(2)	
		a (1N) = 14.(5)	

radical anions. m_0 denotes the FT-ESR intensity of the narrow line 1,5(2,6)-AQDS$^{\bullet 3-}$ radical anion spectrum with a fast generation time constant (<30 ns), and m_1 denotes that part of radical anions that are transfered to the free radical state with the rate constant k_{esc}. The second bracket in eq 6 describes the relaxation of the spin-polarized magnetization to the Boltzmann

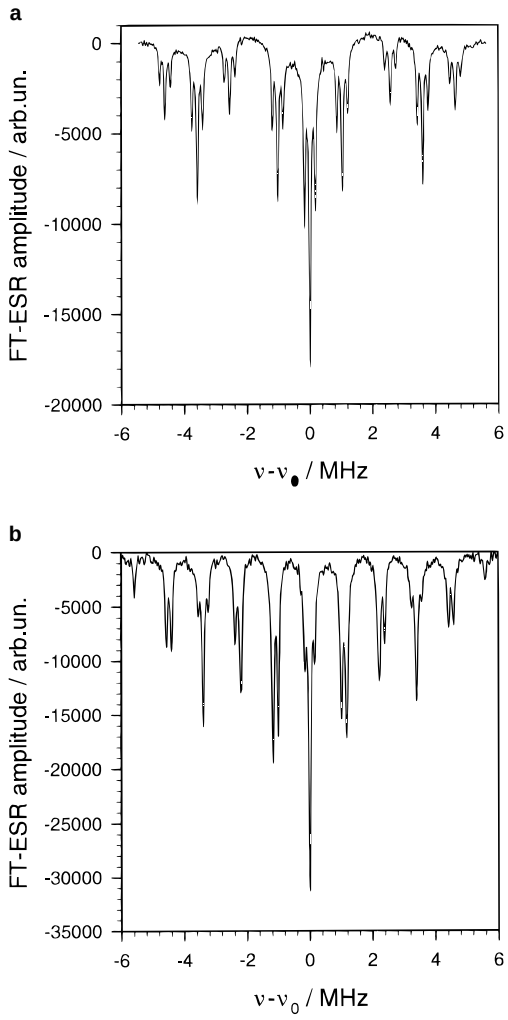

Figure 3. FT-ESR spectra of (a) 1,5-AQDS$^{\bullet 3-}$ and (b) 2,6-AQDS$^{\bullet 3-}$ radical anions after a delay of 32 ns from the laser pulse. The experimental conditions were identical to Figure 1.

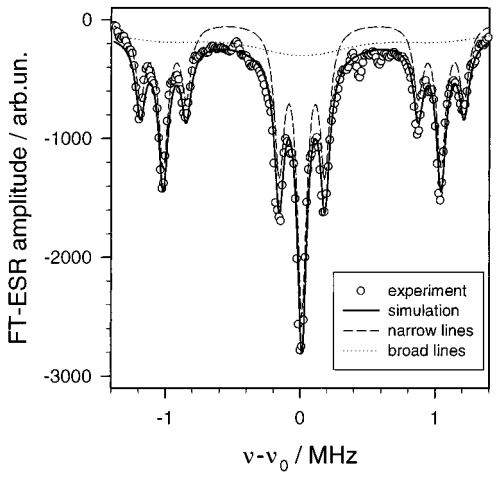

Figure 4. Simulation of the central line groups of 1,5-AQDS$^{\bullet 3-}$ by superposition of two radicals with the same *g* factor and hfs coupling constants (cf. Table 1) and different line widths (84 kHz for narrow line spectrum and 900 kHz for the broad lines).

equilibrium with the polarization factor P and the spin−lattice relaxation time constant T_1. In eq 6 the spin-lattice relaxation T_1 and the generation of free radical anions by the escape step from the Coulomb-coupled radical ion pairs are assumed as independent mechanisms in the dynamics of the spin magnetization. The parameters m_0, m_1, k_{esc}, and T_1, which describe the kinetic behavior of the 1,5-AQDS$^{\bullet 3-}$ and 2,6-AQDS$^{\bullet 3-}$ radical

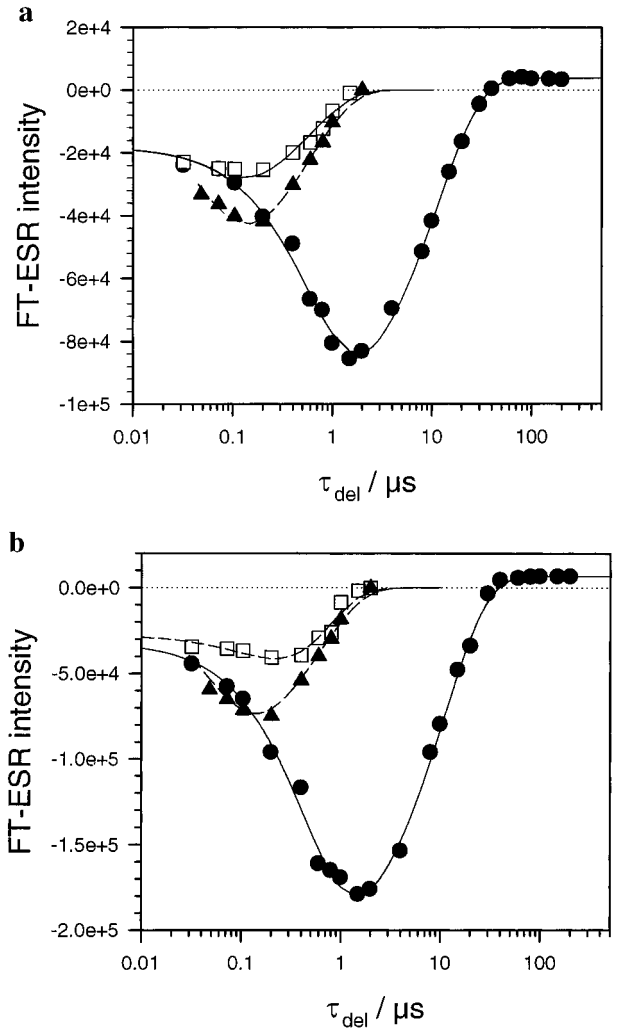

Figure 5. Time dependence of the FT-ESR intensity for the two states of (a) 1,5-AQDS$^{\bullet 3-}$ radical anions and (b) 2,6-AQDS$^{\bullet 3-}$ radical anions and of the radical cation TEA$^{\bullet +}$ at pH = 11: (●) Narrow line spectrum of 1,5(2,6)-AQDS$^{\bullet 3-}$; (□) broad line spectrum of 1,5(2,6)-AQDS$^{\bullet 3-}$; and (▲) TEA$^{\bullet +}$.

TABLE 2: Kinetic Data of the Radical Anions 1,5-AQDS$^{\bullet 3-}$ and 2,6-AQDS$^{\bullet 3-}$ in the Free and Pair State and of the Radical Cation TEA$^{\bullet +}$* in the Pair State (Values Are Valid for [TEA] = 30 mM)

radical	$m_0/(m_0 + m_1)$	k_{esc} [10^6 s^{-1}]	T_1 [μs]
1,5-AQDS$^{\bullet 3-}$/pH=11 (free state)	0.17	1.5 ± 0.2	11 ± 2
1,5-AQDS$^{\bullet 3-}$/pH=14 (free state)	0.49	3.0 ± 0.5	11 ± 2
1,5-AQDS$^{\bullet 3-}$/pH=11 (pair state)	0.17	1.7 ± 0.2	
2,6-AQDS$^{\bullet 3-}$/pH=11 (free state)	0.15	1.5 ± 0.2	11 ± 2
2,6-AQDS$^{\bullet 3-}$/pH=14 (free state)	0.67	9.2 ± 0.5	11 ± 2
2,6-AQDS$^{\bullet 3-}$/pH=11 (pair state)	0.15	1.5 ± 0.2	
TEA$^{\bullet +}$/pH=11		1.7 ± 0.2	
$(CH_3CH_2)_2N-C^{\bullet}HCH_3$/ pH=14		15 ± 3	0.28 ± 0.05

anions, are listed in Table 2. The parameters m_0, m_1, and T_1 are independent of quinone and amine concentrations, indicating that the kinetics of the 1,5-AQDS$^{\bullet 3-}$ and 2,6-AQDS$^{\bullet 3-}$ radical anions are determined by first-order processes. Furthermore, the kinetics of the 1,5(2,6)-AQDS$^{\bullet 3-}$ intensities show a two-phase behavior with a fast process ($k_{esc} > 10^8$ s^{-1}) and a slow rise of the 1,5(2,6)-AQDS$^{\bullet 3-}$ signal. Most important for an

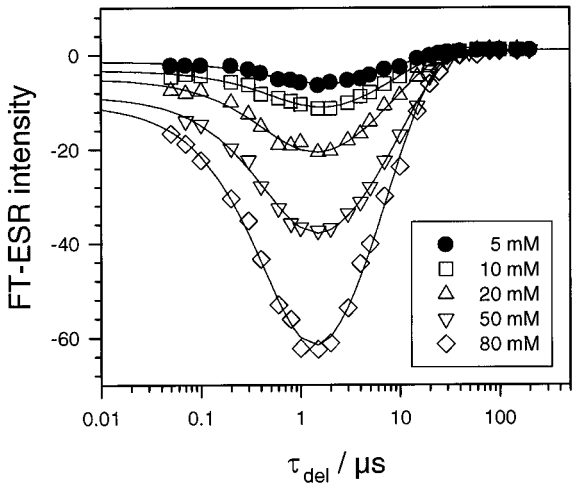

Figure 6. Time dependence of the FT-ESR intensity of the 2,6-AQDS$^{\bullet 3-}$ radical anions for different triethylamine concentrations (5−80 mM TEA). The theoretical lines were calculated with Equ. (6).

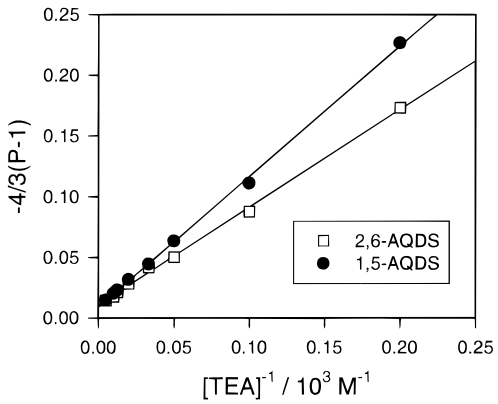

Figure 7. Stern−Volmer plot of the spin polarization of the 1,5(2,6)-AQDS$^{\bullet 3-}$ radical anions in dependence on the reciprocal triethylamine concentration: (●) 1,5-AQDS$^{\bullet 3-}$ and (□) 2,6-AQDS$^{\bullet 3-}$.

assignment of the various signal components is the fact that the slow rise time of isolated 1,5-AQDS$^{\bullet 3-}$ and 2,6-AQDS$^{\bullet 3-}$ radical anions and the decay time of the broad line signal of the 1,5-AQDS$^{\bullet 3-}$ and 2,6-AQDS$^{\bullet 3-}$ radical anions as well as of the radical cations TEA$^{\bullet +}$ are identical. This result indicates that the broad line 1,5(2,6)-AQDS$^{\bullet 3-}$ spectrum is the precursor of the narrow line 1,5(2,6)-AQDS$^{\bullet 3-}$ spectrum. From the line width of the TEA$^{\bullet +}$ radical cations we can conclude that the radical cations are in interaction with radical anions in Coulomb-coupled pairs.

By variation of the triethylamine concentration the competition between spin−lattice relaxation of the spin-polarized quinone triplet and triplet quenching by the electron transfer from amine can be controlled. The time dependence of the total FT-ESR intensity of the 1,5(2,6)-AQDS$^{\bullet 3-}$ radical anions on the amine concentration is shown in Figure 6. This kinetic behavior can be simulated with eq 6 using a polarization factor P and an escape rate constant k_{esc}, which depend on the triethylamine concentration. In Figure 7 the polarization factor P determined with eq 6 is represented in a Stern−Volmer plot. With the equation

$$(4/3)(P-1)^{-1} = P_T^{-1} + (P_T\,{}^3T_1 k_{et}[\mathrm{TEA}])^{-1} \qquad (7)$$

the initial polarization P_T of the quinone triplet state and the product ${}^3T_1 k_{et}$ can be determined (cf. Table 3). An additional detection of the quinone triplet state by its optical spectrum in dependence on the triethylamine concentration allows the direct

TABLE 3: Spin Polarization and Kinetic Parameters of the 1,5(2,6)-AQDS Triplet

	1,5-AQDS$^{\bullet 3-}$	2,6-AQDS$^{\bullet 3-}$
P_T	-200 ± 10	-185 ± 10
$^3T_1$/ns	5.5 ± 0.5	4.6 ± 0.5
D/GHz	8.1 ± 0.5	7.4 ± 0.5
τ_T/ns	140	880
$k_{et}/10^9$ M^{-1} s^{-1}	1.5	2.4

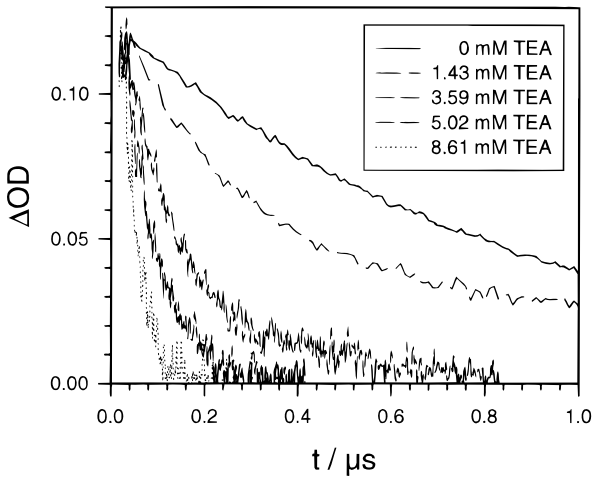

Figure 8. Plots of the optical absorbance at $\lambda = 380$ nm of 2,6-AQDS triplets generated by laser photolysis (10 mJ at 266 nm) in dependence on triethylamine concentration.

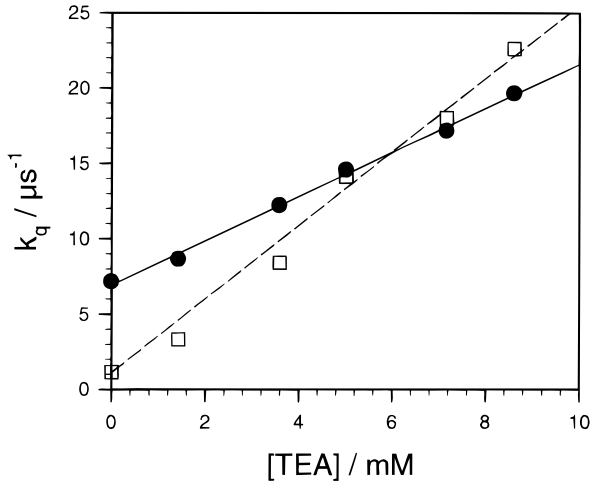

Figure 9. Rate constant of the 1,5(2,6)-AQDS triplet quenching in dependence on the triethylamine concentration: (●) 1,5-AQDS$^{\bullet 3-}$ and (□) 2,6-AQDS$^{\bullet 3-}$.

determination of k_{et}. In Figure 8 the decay of the 2,6-AQDS triplet−triplet extinction at $\lambda = 380$ nm[27] is shown for different triethylamine concentrations. From a plot of the quenching rate constant k_q against the amine concentration (Figure 9) the electron-transfer rate constant k_{et} and the triplet lifetime τ_T can be determined (Table 3). The electron-transfer rate constant is larger by a factor 1.6 for 2,6-AQDS than for 1,5-AQDS, and the triplet lifetime is larger by a factor 6.3 for 2,6-AQDS. The simulation of the signal rise in Figure 6 results in escape rate constants k_{esc} in dependence on the triethylamine concentration shown in Figure 10. The rate constants obtained by the simulation procedure are identical for the 1,5-AQDS$^{\bullet 3-}$ and 2,6-AQDS$^{\bullet 3-}$ radical anions.

In Figure 10 the dependence of the escape rate constant k_{esc} on the triethylamine concentration indicates an amine- or pH-catalyzed proton loss of the TEA$^{\bullet +}$ radical cation.[9] Therefore, we expect a strong influence of the pH on the lifetime of the

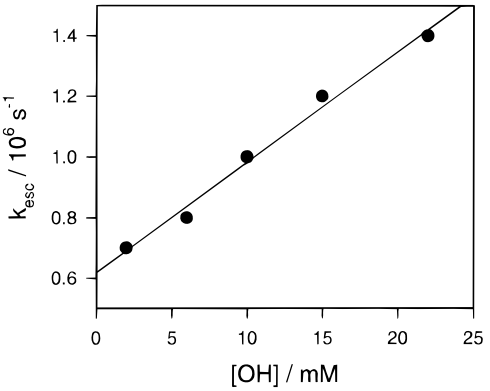

Figure 10. Escape rate constant k_{esc} of 2,6-AQDS$^{\bullet 3-}$ radical anions in dependence on the pH value at different triethylamine concentrations. The results for 1,5-AQDS$^{\bullet 3-}$ radical anions are identical, and therefore, only the results for 2,6-AQDS$^{\bullet 3-}$ radical anions are shown.

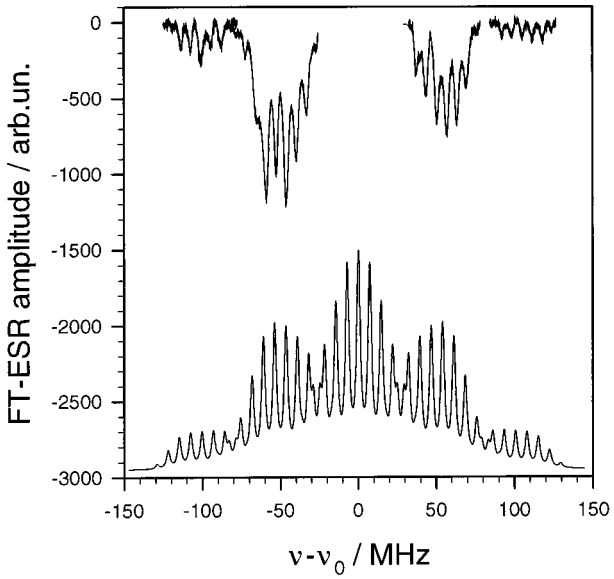

Figure 11. FT-ESR spectrum of the α-aminoalkyl radical $(CH_3CH_2)_2N-C^{\bullet}HCH_3$ at a delay time of 200 ns. Sample: 1 mM 2,6-AQDS with 30 mM TEA at pH = 14. The simulated spectrum was calculated with the hfs coupling constants in Table 1.

radical cations TEA$^{\bullet +}$ and on the buildup kinetics of the 1,5(2,6)-AQDS$^{\bullet 3-}$ radical anions. If we increase the pH to 14, the FT-ESR spectrum of the triethylamine radical cations TEA$^{\bullet +}$ could not be detected, but a new radical was seen. This spectrum is also emissively spin-polarized and could be assigned to α-aminoalkyl radicals $(CH_3CH_2)_2N-C^{\bullet}HCH_3$. In Figure 11 the FT-ESR spectrum of the neutral α-aminoalkyl radicals is shown for the system 2,6-AQDS with 30 mM TEA at pH = 14 and at a delay time of 0.2 μs. The central group of this spectrum is masked by the strong signal from the quinone radical anion. But, the out-of-center line groups can be very well simulated using parameters from the literature.[28] The hfs coupling constants of the α-aminoalkyl radical $(CH_3CH_2)_2N-C^{\bullet}HCH_3$ are listed in Table 1. Our observation clearly proves the transformation of triethylamine radical cations into α-aminoalkyl radicals due to proton loss from the CH_2 group in the α-position.

The kinetic analysis of the FT-ESR intensity of the 1,5-AQDS$^{\bullet 3-}$ and 2,6-AQDS$^{\bullet 3-}$ radical anions shows that the spin polarization and the spin−lattice relaxation does not change with pH, but time profiles at delay times shorter than 1 μs were changed in a characteristic manner:

1. The broad line spectra could only be observed at very short delay times, indicating that the lifetime of the radical ion pairs must be shortened noticeably.

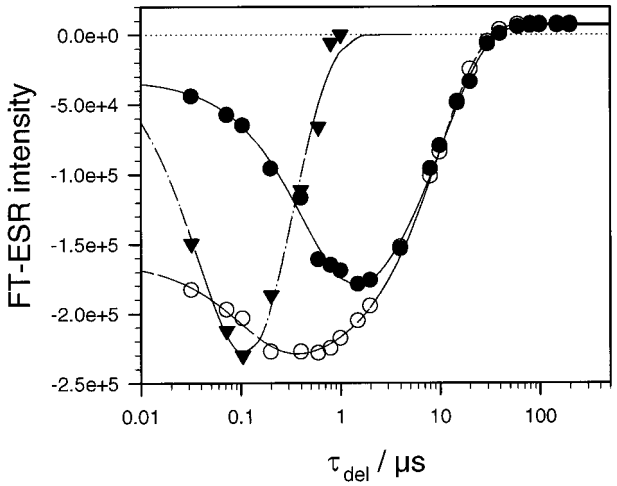

Figure 12. Kinetics of the 2,6-AQDS$^{\bullet 3-}$ radical anion and of the α-aminoalkyl radical $(CH_3CH_2)_2N-C^{\bullet}HCH_3$ under different conditions: (●) pH = 11, (○) pH = 14, and (▼) pH = 14, α-aminoalkyl radical $(CH_3CH_2)_2N-C^{\bullet}HCH_3$. Sample as in Figure 11.

2. The two-phase behavior in the ESR intensities of the radical anions is more clear with a stronger signal with a fast signal rise, which could not be resolved in time by our detection technique. Whereas at pH = 11 the fast signal part is 15−17%, we observed at pH = 14 a fast rising signal part of 50−67% (cf. Table 2).

3. The delayed signal buildup process is faster at pH = 14 than at pH = 11. For 1,5-AQDS the maximum of the signal intensity is achieved at a delay time of 1 μs ($k_{esc} = 3 \times 10^6$ s^{-1}) and for 2,6-AQDS at a delay time of 300 ns ($k_{esc} = 9 \times 10^6$ s^{-1}).

4. The kinetics of the α-aminoalkyl radicals are characterized by a fast buildup time constant of 45 ns and a fast spin−lattice relaxation of the spin polarization with $T_1 = (0.28 \pm 0.05)$ μs (Figure 12). The signal rise time constant is influenced by the experimental time resolution by pulse widths of the laser and the microwave pulses and the buildup kinetics of the radicals. With the experimental time constant the rate constant of the buildup kinetics of the α-aminoalkyl radicals could be estimated to be $k_{esc} = 1.5 \times 10^7$ s^{-1}. At a delay time $\tau_d = 100$ ns the intensities of the α-aminoalkyl radicals and the 2,6-AQDS$^{\bullet 3-}$ radical anions are equal. This means, in these experiments, there is no magnetization that is hidden by line-broadening effects, and therefore, the α-aminoalkyl radicals are detected in the free radical state.

The kinetic results for the slow escape process and the spin−lattice relaxation of all radicals considered are collected in Table 2.

Discussion

In the photoreduction experiments described in this paper all radicals generated from the primary radical ion pairs {1,5(2,6)-AQDS$^{\bullet 3-}$*···TEA$^{\bullet +}$*} could be detected by FT-ESR. Here, we have to distinguish between four different radicals, where two of them belong to the radical anion and two to the triethylamine radical cation TEA$^{\bullet +}$. In the concentration range used (1 mM 1,5(2,6)-anthraquinonedisulfonate with 10−80 mM triethylamine in aqueous solution) the pH was 11 or higher in all samples. At this high pH value both sulfonate groups are fully dissociated.

The FT-ESR spectrum of 1,5(2,6)-AQDS$^{\bullet 3-}$ radical anions can be simulated by a triplet:triplet:triplet splitting with coupling constants listed in Table 1. Apparently, both sulfonate groups are equivalent with the same dissociation state and hydrogen bridged. The hyperfine coupling constants are accounted for in agreement with refs 23 and 24, where the ratio of coupling constants was reported as a(2H,3,7) > a(2H,1,5) > a(2H,4,8) > a(2H,2, 6). An additional coupling to the bridged protons could not be detected. The narrow line width of $\Delta\nu_{1/2} = 84 \pm 5$ kHz indicates that the relaxation times T_1 and T_2 are equal by extreme narrowing.

In the time range up to 2 μs an identical 1,5(2,6)-AQDS$^{\bullet 3-}$ spectrum with a larger line width was observed. The quantitative separation between the narrow and broad line spectra could only be obtained when analyzing LPSVD extrapolated FIDs. The quality of extrapolation can be judged from the excellent base line of these spectra (cf. Figures 3a,b and 4). Both spectra in Figure 4 can be simulated by the same g factor and hfs constants, but the line widths of the narrow and broad line spectra differ by a factor of 10.

Different possibilities for an interpretation of the line-broadening mechanism of the additional signal have been discussed in more detail in refs 9 and 10, invoking two different mechanisms: unresolved additional hfs coupling or restricted molecular diffusional mobility combined with an additional magnetic interaction. An additional hfs coupling might be produced by hydrogen transfer to the anthraquinone triplet to generate neutral 10-hydroxyanthroxyl-9 radicals. The hfs coupling constants of OH groups in neutral quinone radicals are on the order of 1.5−2.0 MHz[29] and depend strongly on the exchange rate of OH protons. This coupling is on the order of the line width of the background spectrum and should result in additional splitting of each line. Furthermore, from unsubstituted AQ it is known[8,9] that the hfs coupling constants in the (2,7)-positions and in the (4,5)-positions enlarge by a factor of 4−5 if semiquinone is protonated to generate neutral quinone radicals. Such a strong spectral change was not observed in the experiments described here. On the other hand, if we consider the deprotonation of a primary generated 10-hydroxyanthroxyl-9 radical, the corresponding FT-ESR spectrum of 1,5(2,6)-AQDS$^{\bullet 3-}$ should appear in the absorption mode because radicals that are generated during the detection time of the FID reverse their phase behavior. Therefore, the broad background spectrum cannot be attributed to neutral 10-hydroxyanthroxyl-9 radicals with an unresolved OH coupling.

The parameters of the triplet polarization P_T and $^3T_1$ determined from the data in Figure 6 are equal for 1,5-AQDS$^{\bullet 3-}$ and 2,6-AQDS$^{\bullet 3-}$ in the error limits (Table 3) and are in the expected region.[9] Also, the zero-splitting parameters D agree very well with the data known from optical-detected zero-field magnetic resonance.[30] The triplet lifetimes obtained from the triplet−triplet absorption (Figures 8, 9) are prolonged by the sulfonate groups in analogy to the data reported by Harriman and Mills[31] for 9,10-anthraquinone and by Hulme et al.[32] for amino-substituted anthraquinones.

The kinetic behavior of the narrow line radical anion spectrum can be interpreted by considering a delayed escape process of 1,5(2,6)-AQDS$^{\bullet 3-}$* from solvent-separated radical ion pairs.[7,9,10] Because of strong magnetic interactions in solvent-separated radical ion pairs in alcoholic solutions as used in refs 7 and 9, the FT-ESR spectra of the radical ions within the pair could not be detected. In these studies, it was found that the lifetime of the radical ion pair is longer in nonpolar solvents than in polar solvents. This can be explained by different dielectric shielding of solvent molecules. Furthermore, it could be shown[9] that the decay of the solvent-separated radical ion pair can be described by a two-component process, in which both the fast decay with a time constant of several tens of nanoseconds and the slow escape process with $k_{esc} = (0.05-1) \times 10^6$ s^{-1} depend

on the amine concentration. In the experiments presented here the line width of the free radical anions 1,5-AQDS$^{\bullet 3-}$ and 2,6-AQDS$^{\bullet 3-}$ is narrower by a factor of 2−4 than in different alcoholic solutions. Whether this behavior is caused by structural or dynamic changes of the radicals cannot be separated here. However, the line width of the broad components shows a similar behavior. Therefore, the broad line background spectra of the 1,5(2,6)-AQDS$^{\bullet 3-}$ radical anions inside the solvent-separated radical ion pair can be detected directly. Their spectroscopic parameters (*g* factor, hyperfine coupling constants) are identical, and the signals appear in emission as expected.

The buildup kinetics of 1,5(2,6)-AQDS$^{\bullet 3-}$ can be described by a two-component process for both pH values considered (cf. eq 6 and Table 2). Whereas the spin polarization and the spin−lattice relaxation do not depend on pH, the escape rate constant k_{esc} and the ratio of fast-to-slow decay of the radical ion pairs depend strongly on the pH of the solution (Table 2). This behavior is similar to the base-catalyzed decay of radical ion pairs in alcoholic solutions described in refs 9 and 10. In alcoholic solutions the lifetime of the primary pairs is controlled by an amine-catalyzed proton loss of the TEA$^{\bullet +}$ radical cation. In the experiments in water described here the lifetime of the radical cation TEA$^{\bullet +}$* is controlled by the OH^- concentration in the solution, as indicated in eq 5 and in Figure 10. With variation of the 2,6-AQDS$^{\bullet 3-}$ concentration (10−80 mM) the pH value of the solution changes from 11.7 to 12.4. In Figure 10 the escape rate constant k_{esc} for 2,6-AQDS$^{\bullet 3-}$ is correlated with the OH concentration. From this linear relation we can conclude that the lifetime of the radical ion pairs is controlled by the OH concentration in the solution, which means the OH concentration controls the lifetime of the amine cation radical inside the radical ion pairs (eq 5). But, this dependence on the OH concentration cannot explain the change of the fast-to-slow escape rate constants from pH = 11 to pH = 14. A possible explanation of this two-phase behavior in the radical anion kinetics might be obtained by radical ion pairs that differ in the content of amine molecules in the first solvation shell. To get more information about this unusual kinetic behavior, experiments with mixed solvents are in progress.

Conclusions

The photoreduction of 9,10-anthraquinone-1,5(2,6)-disulfonate by triethylamine in aqueous solution has been investigated with laser photolysis excitation and detection of the transient radical ions by FT-ESR and optical techniques. Electron transfer from the amine ground state to the quinone triplet as the primary reaction step results in spin-polarized solvent-separated radical ion pairs. With FT-ESR augmented by LPSVD signal analysis, we are able to measure the spectra of isolated 1,5(2,6)-AQDS$^{\bullet 3-}$ radical anions, as well as correlated 1,5(2,6)-AQDS$^{\bullet 3-}$ radical anions and TEA$^{\bullet +}$ radical cations with line widths of $\Delta\nu_{1/2}$ = 0.084, 0.90, and 2.5 MHz, respectively. The *g* factor and the hyperfine coupling constants of 1,5(2,6)-AQDS$^{\bullet 3-}$ are unchanged in the radical ion pair and agree well with the values of the free state 1,5(2,6)-AQDS$^{\bullet 3-}$. Besides line-broadening effects, the kinetic behavior is essential in the assignment of the three spectra to isolated and Coulomb-coupled species. The decay time constants of the pair state radicals agree reasonably well with the rise time of the narrow line 1,5(2,6)-AQDS$^{\bullet 3-}$ spectrum, which we attribute to isolated 1,5(2,6)-AQDS$^{\bullet 3-}$ radical anions in solution. The lifetime of the radical ion pairs can be controlled by the pH value of the solution. At pH = 14 the radical cation TEA$^{\bullet +}$ decays by proton loss in times < 30 ns, resulting in neutral α-aminoalkyl radicals. By switching of the Coulomb attraction in the primary radical ion the lifetime is shorthened noticeably. Therefore, the kinetics of all radical ions monitored describe the lifetime (τ_{Pair} = 0.03−0.66 μs) of solvent-separated radical ion pairs.

Acknowledgment. Prof. K.-P. Dinse (TH Darmstadt) is acknowledged for stimulating discussions. The authors owe a debt of gratitude to the Max-Planck-Society for long-standing support. Financial support for this work was provided by the Deutsche Forschungsgemeinschaft, by the Fonds der Deutschen Chemischen Industrie, and by the Sächsische Ministerium für Wissenschaft und Kultur.

References and Notes

(1) Bowman, M. K. In *Modern Pulsed and Continous-Wave Electron Spin Resonance*; Kevan, L., Bowman, M. K., Eds.; Wiley-Interscience: New York, 1990; Chapter 1 and references therein.
(2) Massoth, R. J. Ph.D. Thesis, University of Kansas, Lawrence, 1987.
(3) Gorcester, J.; Freed, J. H. *J. Chem. Phys.* **1986**, *85*, 5375.
(4) Prisner, T.; Dobbert, O.; Dinse, K. P.; van Willigen, H. *J. Am. Chem. Soc.* **1988**, *110*, 1622.
(5) van Willigen, H.; Levstein, P. R.; Ebersole, M. H. *Chem. Rev.* **1993**, *93*, 173.
(6) Beckert, D.; Schneider, G. *Chem. Phys.* **1987**, *116*, 421
(7) Beckert, D., Plüschau, M.; Dinse, K. P. *J. Phys. Chem.* **1992**, *96*, 3193.
(8) Plüschau, M.; Kroll, G.; Dinse, K. P.; Beckert, D. *J. Phys. Chem.* **1992**, *96*, 8820.
(9) Kausche, T., Säuberlich, J., Trobitzsch, E.; Beckert, D. *Chem. Phys.* **1996**, *208*, 375.
(10) Säuberlich, J.; Brede, O.; Beckert, D. *Acta Chem. Scand.* **1997**, *97*, 602.
(11) Scaiano, J. C. *J. Photochem.* **1973**, *2*, 81.
(12) Cohen, S. G.; Parola, A.; Parsons, G. H. *Chem. Rev.* **1973**, *73*, 141.
(13) Sakaguchi, Y.; Hayashi, H. *Photochem. Photobiol. A: Chem.* **1992**, *65*, 183.
(14) Devadoss, C. W.; Fessenden, R. W. *J. Phys. Chem.* **1991**, *95*, 7253.
(15) Kavarnos, G. J.; Turro, N. J. *Chem. Rev.* **1986**, *86*, 401.
(16) Guttenplan, J. B.; Cohen, S. G. *J. Am. Chem. Soc.* **1972**, *94*, 4040.
(17) Muus, L. T.; Atkins, P. W.; McLauchlan, K. A.; Pedersen, J. B. *Chemically Induced Magnetic Polarization*; Reidel: Dordrecht, 1977; and references therein.
(18) For reviews of CIDEP studies see: (a) McLauchlan, K. A.; Stephens, D. G. *Acc. Chem. Res.* **1988**, *21*, 54. (b) van Willigen, H.; Levstein, P. R.; Ebersole, M. H. *Chem. Rev.* **1993**, *93*, 173.
(19) Säuberlich, J. Ph.D. Thesis, University of Leipzig, Leipzig, 1996.
(20) Zubarev, V.; Brede, O. *J. Chem. Soc., Perkin Trans. 2* **1994**, 1821.
(21) Jeevarajan, A. S.; Fessenden, R. W. *J. Phys. Chem.* **1989**, *93*, 3511.
(22) Stephenson, D. S. *Progr. NMR Spectrosc.* **1988**, *20*, 515.
(23) Vuolle, M.; Makela, R. *J. Chem. Soc., Faraday Trans 1* **1987**, *83*, 51.
(24) Dodd, N. J. F.; Mukherjee, T. *Biochem. Pharmacol.* **1984**, *33*, 379.
(25) Lefkowitz, S. M.; Trifunac, A. D. *J. Phys. Chem.* **1984**, *88*, 77.
(26) Eastland, G. W.; Ramakrishna Rao, D. N.; Symons, M. C. R. *J. Chem. Soc., Perkin Trans. 2* **1984**, 1551.
(27) Linschitz, H. *J. Phys. Chem.* **1983**, *87*, 2536.
(28) McLauchlan, K. A.; Ritchie, A. *J. Chem. Soc., Perkkin Trans. 2* **1984**, 275.
(29) Pedersen, J. A., Ed. *CRC Handbook of EPR Spectra from Quinones and Quinoles*; CRC Press: Boca Raton, 1985.
(30) Kinoshita, M.; Iwasaki *Appl. Spectrosc. Rev.* **1981**, *17*, 1.
(31) Harriman, A.; Mills, A. *Photochem. Photobiol.* **1981**, *33*, 619.
(32) Hulme, B. E.; Land, E. J.; Phillips, G. O. *J. Chem. Soc., Faraday Trans. 1* **1972**, *17*, 2003.